

The nonlinear partial volume effect and computed tomography densitometry of foam and lung

Gerrit J. Kemerink, Rob J. S. Lamers, Guillaume R. P. Thelissen,
and Jos M. A. van Engelsehoven

*Department of Diagnostic Radiology, University Hospital Maastricht, P. Debyelaan 25, P.O. Box 5800,
6202 AZ Maastricht, The Netherlands*

(Received 18 December 1994; accepted for publication 24 April 1995)

A quantitative study was performed to assess the magnitude of the nonlinear partial volume effect (NLPVE) in computed tomography (CT) densitometry of polyethylene foam and lung. This effect arises in materials having density variations on the scale of the sampling area of an individual CT-detector element. It causes a systematic underestimation of the density determined with CT. Foam samples and a resected lung of a goat were imaged with high resolution (20 lp/mm) using a mammography system, and the observed optical density variation in the images was converted into a distribution of pathlengths that x rays penetrate within the solid component of the cellular material. The obtained pathlength distribution was used to calculate the transmission, as seen by a single detector in computed tomography. Comparison with the transmission through homogeneous material of the same thickness gave an estimate of the NLPVE. For the foams studied, the CT-determined density was found to be too low by approximately 0.3%–0.5% due to this effect. Although these density errors are small, in calibrations of a CT scanner they may be of significance. For lung the underestimation of the density was less than 0.1%. These experimentally derived, NLPVE related CT-density errors are 32%–84% of those calculated from a simple model of a cellular solid.

Key words: densitometry, lung density, CT technology

I. INTRODUCTION

The nonlinear partial volume effect^{1,2} (NLPVE) is a well-known cause of streak artifacts between sharp bony edges in computed tomography (CT) of the brain. A less conspicuous corruption of CT numbers exists for all materials that are inhomogeneous on a scale of the order of the sampling area, which is approximately the size of an individual detector in a CT system. Lung, trabecular bone, and also foams that can be used for CT calibrations, contain such structures. The basis for the effect is that the average density in a voxel is linearly related to the average attenuation coefficient (μ), while the measured transmission through a voxel is based on the average of exponentials, containing μ as part of the argument. This leads to a higher transmission than expected on the basis of the average μ , and therefore to an underestimation of the CT number. The effect is not large, but for accurate CT calibrations it may be of relevance. To our knowledge the NLPVE in cellular materials has not been evaluated quantitatively so far. The incentive for the present study was the assessment of factors that affect the accuracy of densitometry of the lungs.

II. MATERIALS AND METHODS

A. Foams and lung

Polyethylene (PE) foams of various densities have been used (PSG, Wellen, Belgium).

These foams have a closed cell structure consisting of polyhedrals.³ Foam types, densities, and estimates of cell size are given in the three leftmost columns of Table I. The low-density polyethylene (LDPE) used in manufacturing these foams has a density of about 0.922 g/cm³.

The lungs studied were from a goat; after resection they were inflated and frozen. All imaging of the lungs was done in this frozen state.

B. Experimental assessment of the nonlinear partial volume effect in cellular solids

The effect of cellular structure on the CT-determined density was investigated by the analysis of projection images of PE foam and lung tissue. The optical density variation, within an area of the image corresponding to the volume that is sampled by a single CT-detector element, was converted to a distribution of pathlengths. The pathlength is defined as the distance a x-ray travels, on its way from the x-ray tube to the film, within the (attenuating) solid component of the cellular structure. This distribution of pathlengths was used to calculate the actual transmission. This transmission, which is affected by the NLPVE, was compared with the calculated transmission through full, void-free material of the same thickness to assess the magnitude of the NLPVE.

The projection images of PE foam and lung were made using a Mammomat-2 mammography system (Siemens, Erlangen, Germany) at 35 kV, with Kodak Min-R H film (Eastman Kodak, Rochester, NY) in a screenless cassette. The size of the focus of the x-ray tube was 0.08 mm and the focus–film distance 760 mm. The beam was diaphragmed to 50×60 mm² at the film position and a minimum foam–film distance of 60 mm was applied to reduce the effect of scattered radiation. The images were digitized using a video camera with a macrolens (JVC CCD TK 870, Victor Company of Japan) and a framegrabber (DT 2853, Data Translation, Marlboro, MA). An area of 5.5×8.5 mm² was converted into a 512×512 matrix with eight-bit resolution (256 gray levels). The

TABLE I. Foam type, density, and foam cell size of the PE foams used, and experimentally determined values for the slope α of the σ_I/l vs $M^{-1/2}$ curve, and the relative error ϵ in the CT-determined attenuation value, as well as α and ϵ calculated according to the simple model.

| Foam type | Density (g/cm ³) | Cell size (mm) | Experiment: α (g/cm ²) ^{1/2} | Experiment: ϵ (%) | Model: α (g/cm ²) ^{1/2} | Model: ϵ (%) |
|-----------|------------------------------|----------------|--|----------------------------|---|-----------------------|
| 28 | 0.023 | 1.8 | 0.185 | -0.32 | 0.33 | -1.00 |
| 34 | 0.027 | 1.5 | 0.224 | -0.47 | 0.30 | -0.83 |
| 35 | 0.037 | 1.5 | 0.234 | -0.51 | 0.30 | -0.82 |
| 65 | 0.059 | 1.5 | 0.186 | -0.32 | 0.29 | -0.80 |
| 95 | 0.095 | 1.0 | 0.195 | -0.35 | 0.23 | -0.51 |
| 100 | 0.109 | 1.0 | 0.211 | -0.42 | 0.23 | -0.50 |
| 150 | 0.164 | 0.8 | 0.173 | -0.28 | 0.20 | -0.36 |

spatial resolution, as found in the digitized images from a line pair phantom, was about 18 lp/mm in the horizontal direction and more than 22 lp/mm in the vertical direction. To investigate the dependence of the NLPVE on foam thickness, an experiment was performed in which stacks of various PE-foam thicknesses, l (10 mm < l < 120 mm) were imaged. The density, ρ_f , of this foam was 0.095 g/cm³. A step wedge of void-free (“full”) PE was imaged for conversion of the gray level to PE thickness.

A second, similar experiment was performed in which the resolution was between 9 (horizontally) and 13 lp/mm (vertically), and the foam thickness between 10 and 330 mm. Images from the goat lung were obtained at three peripheral locations, and ten different regions were digitized and analyzed. Since lung tissue is water equivalent in its attenuation properties,⁴ we imaged water, in cylinders with a 0.1 mm thick plastic foil as a bottom, for conversion of the image gray level to lung thickness. All images were transported to an ICON Quadra 950 (Siemens Gammasonics, Hoffman Estates, IL) for further analysis. On this image processing system the standard deviation in pathlength, σ_I , within a projected area of 1 mm² was determined. This area is approximately the size of the cross section of the volume that is sampled by a single CT detector when using a slice thickness of 1 mm. We calculated σ_I as the root of the difference of the variances found for the cellular solid and the void-free reference material of the same thickness. This correction with the image of the reference material removes, in principle, the effect of noise, film grain, and other instrumental imperfections. In this approach, normal distributions were assumed, based on the finding that fitting histograms with Gaussians yielded generally good fits and essentially the same results for σ_I . Each σ_I was determined as the average of four measurements to reduce the effect of statistical variations.

The fractional difference, ϵ , between the actual and ideal (no NLPVE) path integral of the attenuation coefficient was calculated with expression (9) given below. It turns out that ϵ is also the error in the CT-determined density, as argued hereafter. Attenuation values⁵ used were based on an effective x-ray energy of 73 keV, as measured for our CT system according to the method described by Bergström.⁶

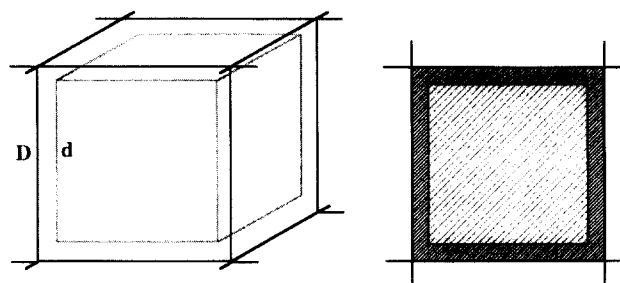


FIG. 1. A cubic cell of a simplified cellular solid. Left: cubic cell with an air-filled cubic cavity, outer size D , and inner size d . Right: top view of a cell. X rays have a chance $p = d^2/D^2$ to pass through a length $(D - d)$ of the solid (incident on a lightly shaded area), and a chance $q = 1 - p$ to pass through a length D (incident on a heavily shaded area).

C. CT experiments

The CT measurements were performed with a Somatom Plus scanner (Siemens, Erlangen, Germany), using our standard high-resolution densitometry protocol: 137 kV, 220 mAs, 1 mm slice thickness and 1 s scanning time. Images were acquired of all foams from Table I. Reconstruction was done with a zoom factor of 5.0 and an ultra-high-resolution filter to realize maximum spatial resolution, as well as with a zoom factor of 1.0 and the standard reconstruction filter. Histograms were made to analyze the CT-number distribution.

D. Calculation of the spread in pathlengths through a simplified cellular solid

An approximate estimate of the effect of the NLPVE can be obtained by considering a simplified cellular solid. Assume the solid to consist of small cubic boxes with cubic, air-filled cavities, neatly ordered in planes, but with the planes stacked randomly with respect to another (Fig. 1). Consider x rays that are penetrating perpendicularly to the planes. The probability that a ray will pass through the air-filled cavity is $p = d^2/D^2$, when D is the outer and d the inner size of the box. The probability that the ray goes through the sidewalls is $q = 1 - p$. When N planes are stacked, the probability $f(n)$ that a ray passes through n air-filled cavities is given by a binomial distribution,

$$f(n) = \binom{N}{n} p^n \cdot q^{N-n}, \quad n = 0, \dots, N. \tag{1}$$

The mean value of n is given by $n_0 = N \cdot p$, the standard deviation by $(N \cdot p \cdot q)^{1/2}$. Rays crossing a box through the cavity penetrate $(D - d)$ of full PE. The other rays, passing through the sidewalls, penetrate a distance D . Setting $x = d/D$, the corresponding average pathlength l_0 within the full material and relative standard deviation (σ_I/l_0) is then given by

$$l_0 = N \cdot D \cdot (1 - x^3) \tag{2}$$

and

$$\frac{\sigma_I}{l_0} = \frac{x^2 \cdot \sqrt{1 - x^2}}{1 - x^3} \cdot \frac{1}{\sqrt{N}}. \tag{3}$$

This simple model predicts the intuitively expected “one over square root of N ” dependence for the relative spread in pathlength. Call the density of foam ρ_f , and suppose M is

the average thickness of the sample in mass per unit area, thus $M = N \cdot D \cdot \rho_f$; then

$$\frac{\sigma_l}{l_0} = \frac{\sqrt{D \cdot \rho_f \cdot x^2 \cdot \sqrt{1-x^2}}}{1-x^3} \cdot \frac{1}{\sqrt{M}} \quad (4)$$

As an example, we will calculate σ_l/l_0 for a hypothetic PE foam, with $\rho_f = 0.095 \text{ g/cm}^3$ and a cubic cell of size 1 mm. Since the full LDPE used for the foams has a density $\rho_m = 0.922 \text{ g/cm}^3$, one then finds $x = d/D = (1 - \rho_f/\rho_m)^{1/3} = 0.9644$ and $\sigma_l/l_0 = 0.233 \cdot M^{-1/2}$.

E. Calculation of the error in CT-determined attenuation coefficients due to the NLPVE

The transmission $T(l_0)$ of x rays through a cellular sample of average thickness l_0 , with l_0 expressed in length units of the full material, can be described as

$$T(l_0) = \frac{T_0}{\sqrt{2\pi \cdot \sigma_l}} \cdot \int_{-\infty}^{+\infty} e^{-\mu \cdot l} \cdot e^{-(l-l_0)^2/(2 \cdot \sigma_l^2)} dl, \quad (5)$$

assuming a normal distribution of pathlengths l around l_0 . In this expression T_0 is the transmission for $l_0 = 0$, μ is the linear attenuation coefficient, and σ_l is the standard deviation of the Gaussian distribution. Note that the assumption of a Gaussian distribution may not hold for small l_0 . The integral can be solved analytically.

When the result is written in the form of an effective path integral, one obtains

$$\ln\left(\frac{T_0}{T(l_0)}\right) = \mu \cdot l_0 - \frac{\mu^2 \cdot \sigma_l^2}{2} \quad (6)$$

Assuming that

$$\frac{\sigma_l}{l_0} \equiv \frac{\alpha}{\sqrt{M}} = \frac{\alpha}{\sqrt{l_0 \cdot \rho_m}}, \quad (7)$$

as found in the present experiments and according to the simple model, this result can be written as

$$\ln\left(\frac{T_0}{T(l_0)}\right) = \mu \cdot l_0 \cdot \left(1 - \frac{\alpha^2 \cdot (\mu/\rho_m)}{2}\right). \quad (8)$$

Note that (μ/ρ_m) is simply the mass attenuation coefficient. In absence of the NLPVE the path integral would have been $\ln(T_0/T(l_0)) = \mu \cdot l_0$.

From this last expression and (8), it can be seen that the fractional underestimation of the path integral is

$$\epsilon = \frac{-\alpha^2 \cdot (\mu/\rho)}{2}, \quad (9)$$

with (μ/ρ) the mass attenuation coefficient. This result is independent of l_0 , therefore, all path integrals are affected by the same fractional error ϵ . Consequently, the reconstructed attenuation coefficient, or equivalently the density, will be in error by this same fraction, as the CT has no way of knowing whether the higher measured transmission is due to a less dense homogeneous object or the NLPVE in a foam.

III. RESULTS

Figure 2 shows as an example the histograms of the gray levels within regions of 1 mm^2 drawn in images of 81 mm

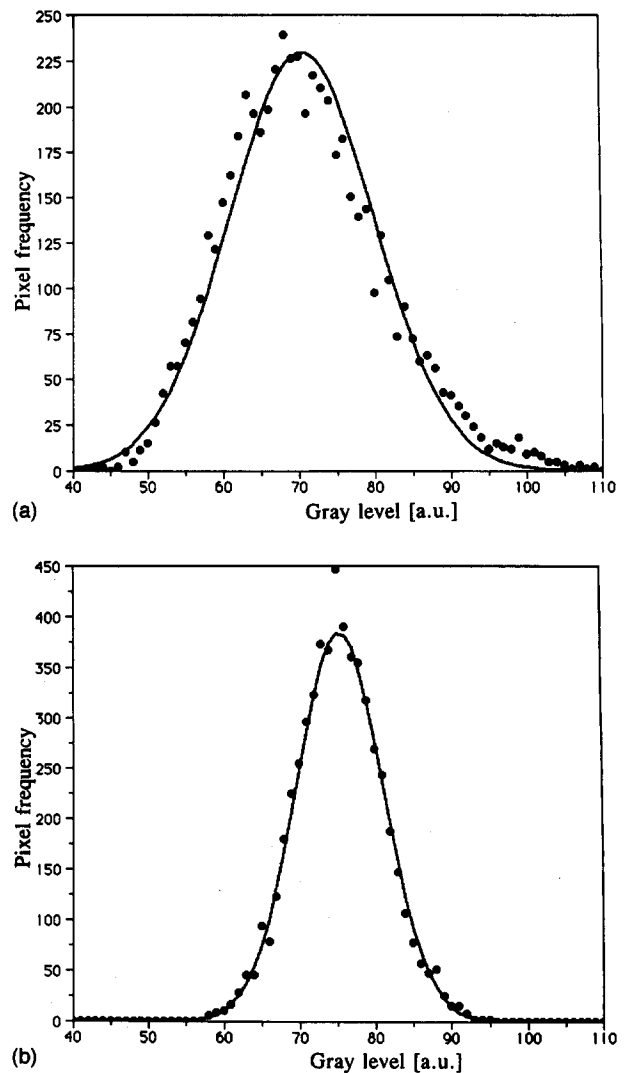


Fig. 2. Histograms of gray levels within a region of 1 mm^2 for an image of PE Foam-95 (0.77 g/cm^2) (a), and full PE of slightly larger thickness (0.86 g/cm^2) (b). Both histograms have been fitted with a Gaussian.

thick Foam-95 (0.77 g/cm^2) and full PE of slightly larger thickness (0.86 g/cm^2). Both curves have been fitted with Gaussians. The square root of the difference of their variances is a measure for the spread in pathlength.

Figure 3 displays the relative spread in pathlength, σ_l/l , versus the inverse of the square root of the foam stack thickness, $M^{-1/2}$, with M expressed as mass per unit area (g/cm^2) [see expression (4) above]. The data have been fitted with a straight line; the fit, passing nearly through the origin, appears to be satisfactorily. The slope, α , is $0.198 (\text{g/cm}^2)^{1/2}$, the y offset -0.003 . When the line was forced to pass through the origin, the slope changed to $0.195 (\text{g/cm}^2)^{1/2}$.

The slope according to the simple model is $0.233 (\text{g/cm}^2)^{1/2}$.

For the data obtained with a spatial resolution of about 10 lp/mm, instead of 20 lp/mm, the slope was $0.176 (\text{g/cm}^2)^{1/2}$ and the y offset -0.024 . A line through the origin has a slope of $0.153 (\text{g/cm}^2)^{1/2}$. In one case the area that was analyzed was varied: for a region of $0.5 \times 0.5 \text{ mm}^2$, a 9% lower value of σ_l/l was found, and for a $2 \times 2 \text{ mm}^2$ a 22% higher value.

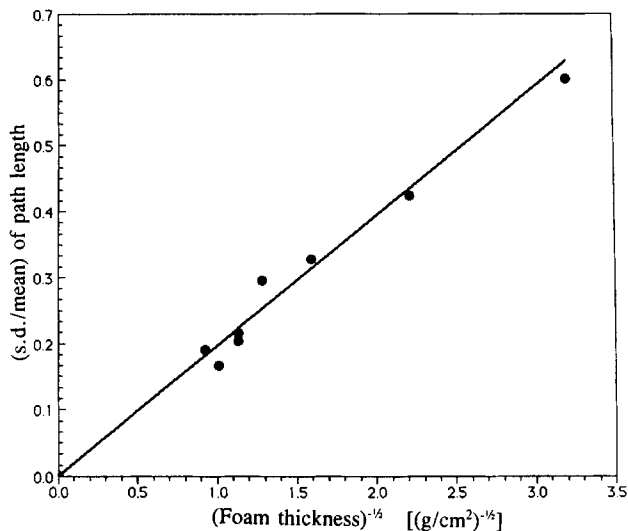


FIG. 3. Relative standard deviation in pathlength σ_l/l_0 that x rays travel within the solid component of PE Foam-95 as a function of one over the square root of the foam thickness $M^{-1/2}$.

For the other foams of Table I, only one image was taken from a sample, with a thickness between 110 and 134 mm. Table I shows the experimental results for α in the relation $\sigma_l/l = \alpha \cdot M^{-1/2}$, as well as the fractional error ϵ in the CT-determined attenuation value. Results according to the model are also shown, assuming a cubic cell with a size equal to the diameter of the polyhydrons, as given in Table I.

The results obtained for lung are shown in Fig. 4. The slope of a line through the origin is $0.068 \text{ (g/cm}^2\text{)}^{1/2}$.

Finally, Fig. 5 shows the histograms of the CT numbers obtained for Foam-28 after reconstruction with the ultra-high-resolution filter and a zoom factor of 5.0, as well as after reconstruction with the standard reconstruction filter and a zoom factor of 1.0.

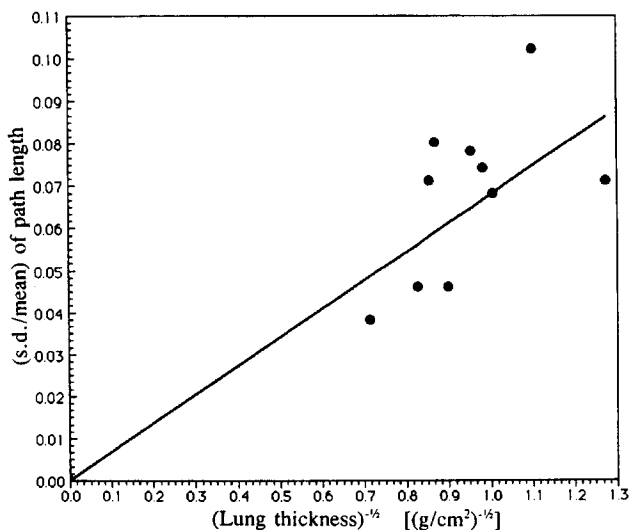


FIG. 4. Relative standard deviation in pathlength σ_l/l_0 that x rays travel within the solid component of the lung as a function of one over the square root of the lung thickness $M^{-1/2}$.

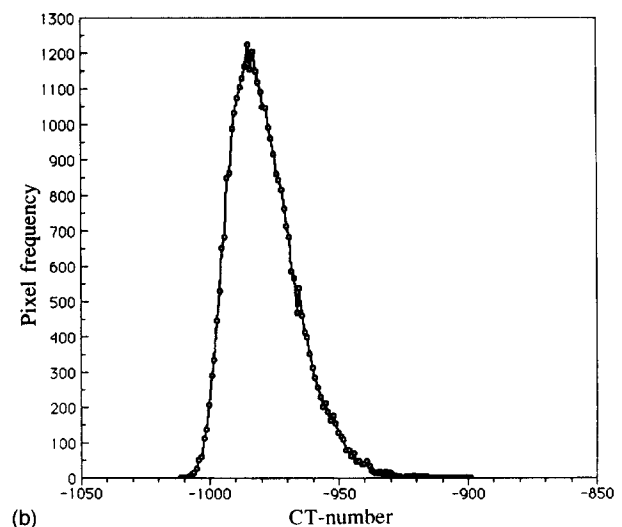
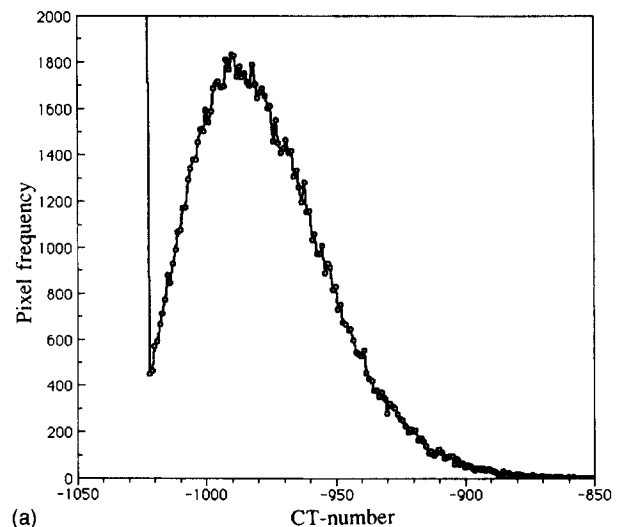


FIG. 5. Histograms of CT numbers of images of PE Foam-28 acquired at 137 kV, 220 mAs, 1 mm slice thickness and 1 s scanning time. (a) Reconstructed with a zoom factor of 5.0 and the ultra-high-resolution filter. The truncation of the histogram at a CT number of -1023 HU is due to the way CT numbers are stored as 12 bit integers in this scanner.⁷ (b) Reconstructed with a zoom factor of 1.0 and the standard filter.

IV. DISCUSSION

A direct measurement of the nonlinear partial volume effect (NLPVE) by comparing x-ray transmission through a void-free solid and a foam with the same mass per unit area is extremely difficult: (i) the effect is small; (ii) it is very hard to determine the mass per unit area of a foam with sufficient accuracy; and (iii) the size of the samples is very different, resulting in different scattering conditions.

The procedure adopted here relies on the high sensitivity of measuring differences in pathlengths using low-energy x rays and a high resolution imaging system, and the subsequent calculation of the (small) NLPVE from the measured pathlength distribution.

The model that was introduced illustrates some properties of x-ray transmission through a simplified cellular solid. It deviates from reality in several aspects, however, (i) in a real foam there is randomness in all directions, with sometimes

some anisotropy; (ii) PE foam has closed cells in the form of polyhedrons, not cubes; (iii) there is some variation in cell size; and (iv) a large part of the mass is concentrated in the edges where faces of the polyhedrons meet.

The model predicted a $M^{-1/2}$ dependence for σ_1/l , and the same dependence appears to exist for real foams. This finding may also be understood by a more phenomenological argument. Consider a slice of foam with a thickness M , such that it is a representative sample of the material. When such a layer has a normal distribution of pathlengths, adding another layer leads to a distribution in pathlengths that is given by the convolution of two Gaussians, resulting in the observed $M^{-1/2}$ dependence. Clearly the relation may not hold for very thin layers of foam. The condition that the distributions are normal appeared to be reasonably well fulfilled: fitting the histograms with Gaussians yielded acceptable fits (Fig. 2) and very similar values for σ_1/l .

The slope of the measured σ_1/l vs $M^{-1/2}$ curve is smaller than according to the simple model: 0.195 compared to 0.233 (g/cm^2)^{1/2}. This might be expected because the possible variation in pathlength has nearly been maximized in the model by distinguishing only two largely different paths in each single cell. The model prediction for σ_1/l may therefore probably be considered as an upper limit for all conceivable foams of the same density and cell size.

A problem of the present investigation is the limited spatial resolution of the projection images made with the mammography unit. The highest resolution achieved was about 20 lp/mm, which corresponds approximately with a FWHM of 50 μm of the point spread function.

In the discussion of the effect of this limited resolution we will first concentrate on the results for Foam-95. Foam-95 has a cell size of about 1.0 mm. Gibson and Ashbe³ [Chap. 2, Table 2.1, the tetrakaidecahedron, and formulas (2.19a and (2.19b)] give expressions to calculate the thickness of the faces (t_f) and edges (t_e) of the polyhedrons. Edges are the lines where faces meet, and where generally significant accumulation of material occurs. The fraction, ϕ , of the total mass residing in the edges is unknown but can indirectly be estimated by measuring the ratio of t_e/t_f . The ratio for t_e/t_f we found by examining a thin foam section under a microscope, was between 3 and 6, and consequently ϕ is calculated as lying between 0.5 and 0.7, t_f between 25 and 15 μm , and t_e between 74 and 87 μm . From these numbers it is concluded that, due to the limited resolution, the thickness of a single edge estimated from the images would be too low by about 15%. In the experiment with a resolution of about 10 lp/mm this would be 35%–40%. The actual image is, of course, a superposition of projections of many edges and faces. The faces are very thin, but they have considerable size, the x rays will generally be obliquely incident, and they contain only a part (30%–50%) of the mass, so the underestimation of the spread in pathlength due to the limited resolution will not be too severe for this mass component. Some idea of the influence of spatial resolution may also be gained by comparison of the results from the 10 and 20 lp/mm experiments. By improving the resolution by about a factor of 2, the slope of the σ_1/l vs $M^{-1/2}$ curve increased by about 20%, from 0.153 to 0.195 (g/cm^2)^{1/2}. The latter value is still

16% lower than the model value, which might be considered as an upper limit for a foam of this density and cell size.

We conclude from this discussion of Foam-95 that we underestimate σ_1/l , but probably by not more than 10%–20%.

For the other foams $t_e(t_f)$ ranges from 64 μm (9 μm) for Foam-34, to 160 μm (28 μm) for Foam-150, not relevantly different from Foam-95. The fraction by which the CT-estimated attenuation coefficient of the foams is wrong ranges between –0.28% for Foam-150 and –0.51% for Foam-35. These values are between 32% and 84% of those according to the simple model.

The effect of the size of the sampled area on the spread in pathlengths depends on the cell size and sample thickness. For one sample of Foam-95, decreasing the sampled area from 1 to 0.25 mm² led to a nearly 20% smaller density error, while increasing the area to 4 mm² led to a 50% larger density error. Generally one would expect, when a representative part of the foam is within the probed area, that a further increase of beam size has minor influence. The effect has not been studied in more detail, however.

Although the density errors generally appear to be small, for slightly coarser foams, the error may increase significantly because of the quadratic dependence of ϵ on α .

In most practical cases, the density errors presently found will be negligible, but in CT calibrations where several foams are used with densities known to about 1% accuracy, and where CT numbers can be averaged over large areas, a correction for this systematic error may be appropriate.

We have discussed the influence of the NLPVE on the average attenuation coefficient of the mixture of air and PE. But is an average attenuation coefficient indeed observed in CT? The high-resolution CT images of all foams revealed broad unimodal histograms, with no peaks at the CT numbers, corresponding to either air density or the density of full PE, not even for Foam-28, which has a cell size of about 1.8 mm (Fig. 5). Clearly, all structures are affected by the partial volume effect, even at the highest possible resolution [Fig. 5(a)]. Using the standard reconstruction filter, as is normally done in densitometry of the lungs, the distributions are considerably narrower [Fig. 5(b)]. Clearly, for CT the average attenuation coefficient of the air–PE mixture, constituting these foams, is a suitable parameter.

We end the discussion of the NLPVE for PE foams, noting another practical problem of (both full and foamed) PE in having attenuation properties that are not equivalent to those of water. This fact leads, in scanners using a water-based beam hardening correction, to an underestimation of the density. The magnitude of the effect can be found from simulations.⁷ Since this problem is not related to the NLPVE, it will not be discussed here.

The anatomy of lungs⁸ is much more complicated than that of foam. The equivalent of a foam cell is the alveolus, about 150–200 μm in diameter, with walls of the order of 10 μm . A larger structure present is the bronchial tree, with diameters of several millimeters down to about 0.5 mm. Similarly, there is an arterial tree closely following the bronchial tree, having diameters of several millimeters down to several μm for the capillaries in the alveolar walls. Finally,

the lung contains septa with a thickness of the order of 100 μm , with which the venous vasculature appears to be associated. As with the foams, the alveolar walls have a thickness that is well below the spatial resolution of our experiments. The other, larger structures should be imaged more or less correctly. The experiments yielded an average slope of $0.068 (\text{g}/\text{cm}^2)^{1/2}$ for the σ_1/l vs $M^{-1/2}$ curve, which, as with the foams, will be a lower limit. The corresponding underestimation of the attenuation coefficient in CT would be 0.04%.

For healthy persons at 10% and 90% of the vital capacity densities of 0.22 and 0.15 g/cm^3 have been reported.⁹ Assuming an average alveolar diameter of 175 μm of the distended lung, one finds according to the simple model values for α of 0.086 and 0.098 $(\text{g}/\text{cm}^2)^{1/2}$ at 10% and 90% of the vital capacity, with corresponding underestimations of the density of 0.07% and 0.09%. The values for lung are considerably lower than for foam, because for a given ρ_f/ρ_m ratio ϵ scales linearly with the cell size.

V. CONCLUSION

A method was presented to quantitate experimentally the nonlinear partial volume effect (NLPVE) in cellular solids. The results for PE foam indicate that the average attenuation coefficient as estimated by CT is too low by a fraction of approximately 0.3%–0.5%, dependent on the foam. For lung the underestimation is less than 0.1%, and certainly negligible when compared to other uncertainties present in clinical densitometry. A simple theoretical model for a cellular material was developed that might be used to roughly estimate the magnitude of the NLPVE.

ACKNOWLEDGMENTS

The authors would like to thank H. M. W. Hamers, Department of Psychiatry and Neuropsychology of the University of Limburg, Maastricht, for putting the framegrabber system at our disposal and his help in using it, Ir. G. F. J. LeDoux of DSM, Geleen, for his expert advice on foams and polyethylene and J. J. M. Ackermans of our hospital for his help in the nonstandard imaging with the mammography system.

¹P. M. Joseph, "Artifacts in computed tomography," in *Radiology of the Skull and Brain: Technical Aspects of Computed Tomography*, edited by T. H. Newton and D. G. Potts (The C. V. Mosby Company, St. Louis, MO, 1981), pp. 3956–3992.

²G. H. Glover and N. J. Pelc, "Nonlinear-partial volume artifacts in x-ray computed tomography," *Med. Phys.* **7**, 238–248 (1980).

³L. J. Gibson and M. F. Ashby, *Cellular Solids: Structure and Properties* (Pergamon, Oxford, 1988).

⁴ICRU-Report No. 44. "Photon, electron, proton and neutron interaction data for body tissues," International Commission on Radiation Units and Measurements, 7910 Woodmont Avenue, Bethesda, MD 20814, 1989.

⁵M. J. Berger and J. H. Hubbell, "XCOM: Photon cross sections on a personal computer, (Version 1.2, 1987)," Center for Radiation Research, National Bureau of Standards, Gaithersburg, MD 20899.

⁶M. Bergström, "Performance evaluation of scanners," in Ref. 1, pp. 4212–4227.

⁷G. J. Kemerink, R. J. S. Lamers, G. R. P. Thelissen, and J. M. A. van Engelshoven, "CT-densitometry of the lungs: Scanner performance," to appear in *J. Comput. Assist. Tomogr.*

⁸C. Kuhn, "Normal anatomy of the lung," in *Pathology of the Lung*, edited by W. M. Thurlbeck (Thieme Medical Publishers, New York, 1988), pp. 11–50.

⁹R. J. Lamers, G. R. Thelissen, A. G. Kessels, E. F. Wouters, and J. M. van Engelshoven, "Chronic obstructive pulmonary disease: Evaluation with spirometrically controlled CT lung densitometry," *Radiology* **193**, 109–113 (1994).